Tenth SPE Comparative Solution Project: A Comparison of Upscaling Techniques

M.A. Christie, SPE, Heriot-Watt U., and **M.J. Blunt,** SPE, Imperial College

Summary

This paper presents the results of the 10th SPE Comparative Solution Project on Upscaling. Two problems were chosen. The first problem was a small 2D gas-injection problem, chosen so that the fine grid could be computed easily and both upscaling and pseudoization methods could be used. The second problem was a waterflood of a large geostatistical model, chosen so that it was hard (though not impossible) to compute the true fine-grid solution. Nine participants provided results for one or both problems.

Introduction

The SPE Comparative Solution Projects provide a vehicle for independent comparison of methods and a recognized suite of test data sets for specific problems. The previous nine comparative solution projects[1–9] have focused on black-oil, compositional, dual-porosity, thermal, or miscible simulations, as well as horizontal wells and gridding techniques.

The aim of the 10th Comparative Solution Project was to compare upgridding and upscaling approaches for two problems. Full details of the project, and data files available for downloading, can be found on the project's Web site.[10]

The first problem was a simple, 2,000-cell 2D vertical cross section. The specified tasks were to apply upscaling or pseudoization methods and to obtain solutions for a specified coarse grid and a coarse grid selected by the participant.

The second problem was a 3D waterflood of a 1.1-million-cell geostatistical model. This model was chosen to be sufficiently detailed so that it would be hard, though not impossible, to run the fine-grid solution and use classical pseudoization methods.

We will not review the large number of upscaling approaches here. For a detailed description of these methods, see any of the reviews of upscaling and pseudoization techniques, such as Refs. 11 through 14.

Description of Problems

Model 1. The model is a two-phase (oil and gas) model that has a simple 2D vertical cross-sectional geometry with no dipping or faults. The dimensions of the model are 2,500 ft long×25 ft wide×50 ft thick. The fine-scale grid is 100×1×20, with uniform size for each of the gridblocks. The top of the model is at 0.0 ft, with initial pressure at this point of 100 psia. Initially, the model is fully saturated with oil (no connate water). Full details are provided in Appendix A.

The permeability distribution is a correlated, geostatistically generated field, shown in **Fig. 1.** The fluids are assumed to be incompressible and immiscible. The fine-grid relative permeabilities are shown in **Fig. 2.** Residual oil saturation was 0.2, and critical gas saturation was 0. Capillary pressure was assumed to be negligible in this case. Gas was injected from an injector located at the left of the model, and dead oil was produced from a well to the right of the model. Both wells have a well internal diameter of 1.0 ft and are completed vertically throughout the model. The injection rate was set to give a frontal velocity of 1 ft/D (about 0.3 m/d or 6.97 m^3/d), and the producer is set to produce at a constant bottomhole pressure limit of 95 psia. The reference depth for the bottomhole pressure is at 0.0 ft (top of the model).

This paper (SPE 72469) was revised for publication from paper SPE 66599, first presented at the 2001 SPE Reservoir Simulation Symposium, Houston, 11–14 February. Original manuscript received for review 19 April 2001. Revised manuscript received 21 May 2001. Paper peer approved 31 May 2001.

The specified tasks were to apply an upscaling or pseudoization method in the following scenarios.

1. 2D: 2D uniform 5×1×5 coarse-grid model.
2. 2D: 2D nonuniform coarsening, maximum 100 cells.

Directional pseudorelative permeabilities were allowed if necessary.

Model 2. This model has a sufficiently fine grid to make the use of any method that relies on having the full fine-grid solution almost impossible. The model has a simple geometry, with no top structure or faults. The reason for this choice is to provide maximum flexibility in the selection of upscaled grids.

At the fine geological model scale, the model is described on a regular Cartesian grid. The model dimensions are 1,200×2,200×170 ft. The top 70 ft (35 layers) represent the Tarbert formation, and the bottom 100 ft (50 layers) represent Upper Ness. The fine-scale cell size is 20×10×2 ft. The fine-scale model has 60×220×85 cells (1.122×10^6 cells). The porosity distribution is shown in **Fig 3.**

The model consists of part of a Brent sequence. The model was originally generated for use in the PUNQ project.[15] The vertical permeability of the model was altered from the original; originally, the model had a uniform k_V/k_H across the whole domain. The model used here has a k_V/k_H of 0.3 in the channels and a k_V/k_H of 10^{-3} in the background. The top part of the model is a Tarbert formation and is a representation of a prograding near-shore environment. The lower part (Upper Ness) is fluvial. Full details are provided in Appendix B.

Participants and Methods

Chevron. Results were submitted for Model 2 using CHEARS, Chevron's in-house reservoir simulator. They used the parallel version and the serial version for the fine-grid model and the serial version for the scaled-up model.

Coats Engineering Inc. Runs were submitted for both Model 1 and Model 2. The simulation results were generated with SENSOR.

GeoQuest. A solution was submitted for Model 2 only, with coarse-grid runs performed using ECLIPSE 100. The full fine-grid model was run using FRONTSIM, a streamline simulator,[16] to check the accuracy of the upscaling. The coarse-grid models were constructed with FloGrid, a gridding and upscaling application.

Landmark. Landmark submitted entries for both Model 1 and Model 2 using the VIP simulator. The fine grid for Model 2 was run with parallel VIP.

Phillips Petroleum. Solutions were submitted for both Model 1 and Model 2. The simulator used was SENSOR.

Roxar. Entries were submitted for both Model 1 and Model 2. The simulation results presented were generated with the black-oil implicit simulator Nextwell. The upscaled grid properties were generated using RMS, specifically the RMSsimgrid option.

Streamsim. Streamsim submitted an entry for Model 2 only. Simulations were run with 3DSL, a streamline-based simulator.[17]

TotalFinaElf. TotalFinaElf submitted a solution for Model 2 only. The simulator used for the results presented was ECLIPSE; results were checked with the streamline code 3DSL.

U. of New South Wales. The U. of New South Wales submitted results for Model 1 only, using CMG's IMEX simulator.

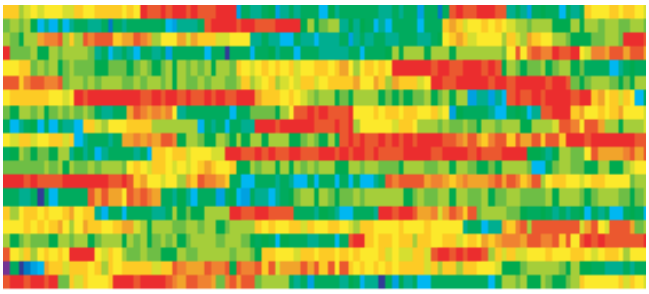

Fig. 1—Log permeability field, Model 1.

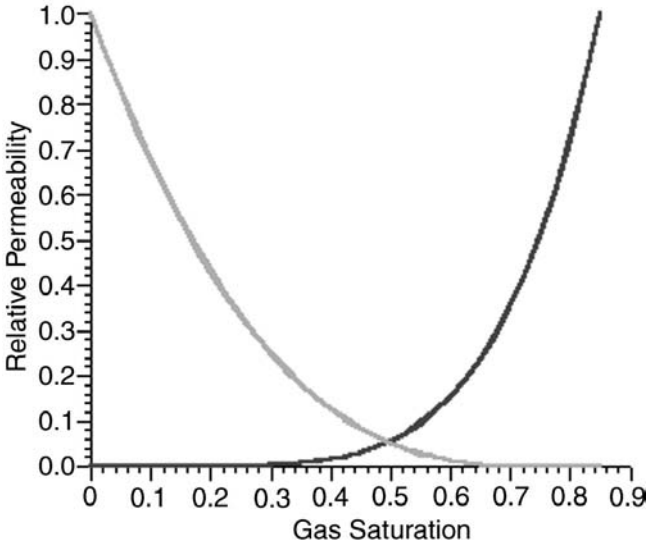

Fig. 2—Relative permeabilities for Model 1.

Results

Model 1. ***Fine-Grid Solution.*** All participants were able to compute the fine-grid solution, and the solutions from the different simulators used were very close, as shown in **Fig. 4.** The U. of New South Wales' fine-grid solution departs slightly from the other fine-grid solutions; it was not possible to locate the source of this discrepancy in the short time between receiving this solution and the paper submission deadline.

Upscaled Solutions. Participants were asked to generate solutions on a 5×5 grid and on a grid of their choice with a maximum of 100 cells. The reason for the choice of the 5×5 grid was that, with that grid size, the coarse-grid boundaries fall on high-permeability streaks, which is generally a problem for upscaling methods that don't compute the fine-grid solution.

The solutions submitted for the 5×5 grid used single-phase upscaling only (Roxar) or single-phase upscaling plus regression-based pseudoization of relative permeabilities (Coats, Phillips, and Landmark). The solutions with pseudorelative permeabilities are very close to the fine-grid solution, and Roxar's solution using only single-phase upscaling shows a significant discrepancy **(Fig. 5).**

A second set of solutions was presented by some participants (shown in **Fig. 6**). Here, Roxar used single-phase upscaling in conjunction with a streamline approach to generate local grid refinements (with a total of 96 cells) that captured the details of flow in the early-, mid-, and late-time regions. Coats showed that good results also could be obtained with homogeneous absolute permeability and no alteration of relative permeability, and Phillips showed that good results could be obtained from a 6×2 grid. The U. of New South Wales' solution was based on a global upscaling and upgridding approach that attempts to minimize the variance of permeability within a cell.[18] Their solution is close to their fine-grid solution, although the difference between their fine-grid solution and the other fine-grid solutions tends to make their

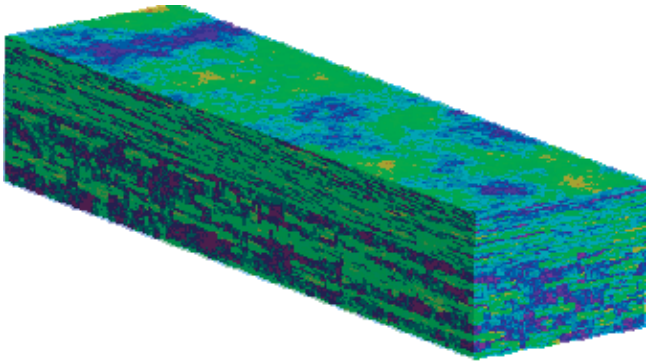

Fig. 3—Porosity field, Model 2.

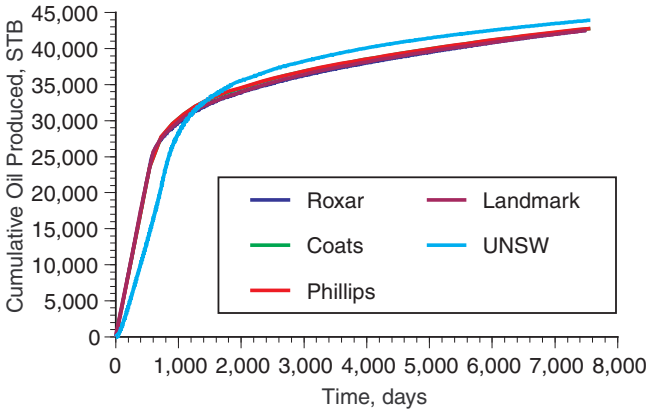

Fig. 4—Comparison of fine-grid results, Model 1.

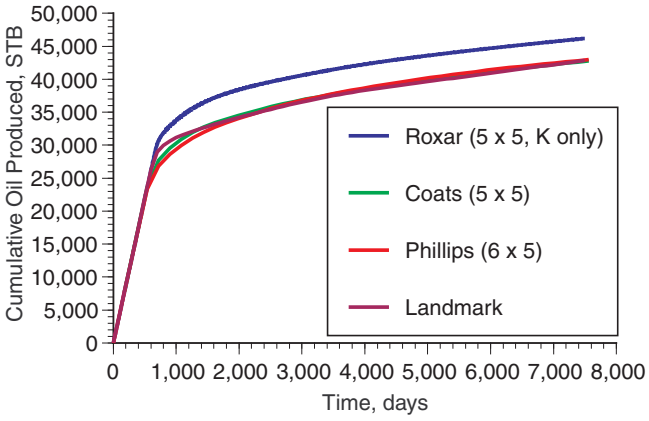

Fig. 5—Comparison of 5×5 results, Model 1.

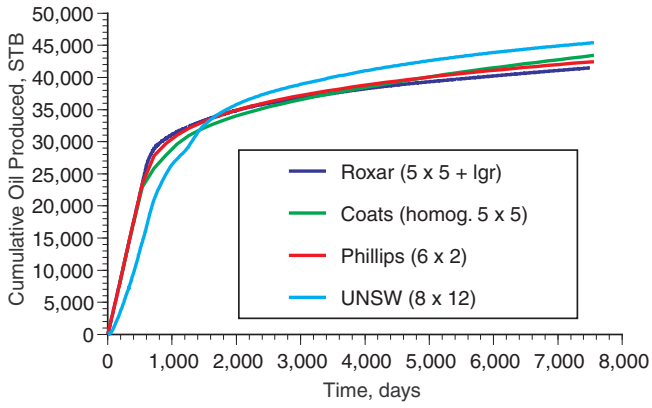

Fig. 6—Comparison of alternative models for Model 1.

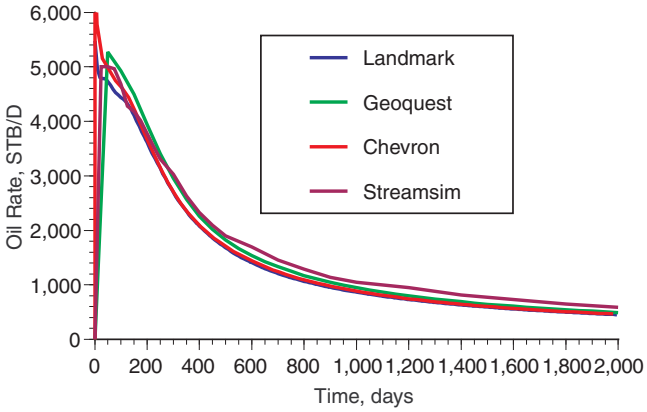

Fig. 7—Comparison of fine-grid field oil rate, Model 2.

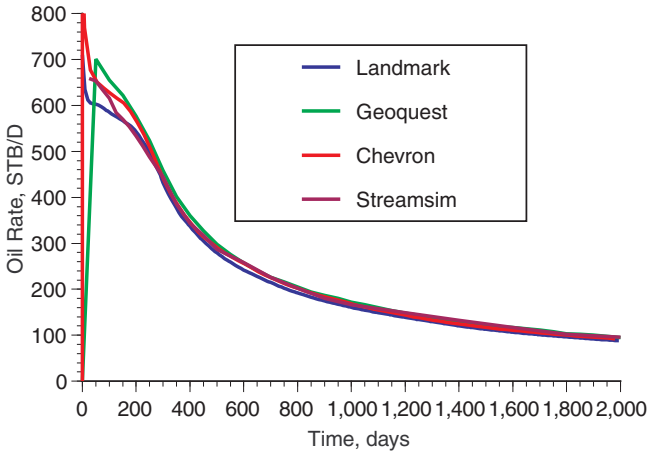

Fig. 8—Comparison of fine-grid Producer 1 oil rate, Model 2.

method appear to perform less satisfactorily. After the paper was presented, CMG ran the Model 1 fine-grid solution with IMEX and obtained fine-grid results identical to the other participants, indicating a minor discrepancy in the U. of New South Wales input data set.

Model 2. ***Fine-Grid Solution.*** Five participants provided fine-grid results as well as an upscaled solution. Landmark and Chevron ran the full fine grid on a parallel reservoir simulator. GeoQuest and Streamsim provided results using streamline codes. (TotalFinaElf also provided streamline results using 3DSL; we have not shown their production curves as they are the same as Streamsim's.) A comparison of the fine-grid results is shown in **Figs. 7 through 10.** All the figures show very good agreement between all four fine-grid submissions. Although only Producer 1 well plots are shown here for reasons of space, plots of the remaining well rates and water cuts show equally high levels of agreement between the four fine-grid solutions. The differences that occur are likely to be caused by different timesteps early on, where the production rate is very sensitive to the transient pressure response, or by different treatment of the injection well, which was at the corner of four cells in the fine model, leading to different injectivity indices.

Upscaled Solutions. There were two methodologies used to generate the upscaled solutions. Some participants used finer-scale information in some way, and then history-matched a coarser grid to the finer-grid results. Others made no use of fine-scale flow information and used standard, well-documented upscaling procedures to compute upscaled grids and upscaled effective permeabilities.

Landmark, Phillips Petroleum, and Coats Engineering used some level of fine-scale flow information to determine upscaled relative permeabilities for a coarse-grid model. All other participants used some form of single-phase upscaling, some in conjunction with flow-based upgridding. There were significant variations in final grid sizes and upscaling approaches chosen.

Landmark ran the full fine-grid model, then used flow-based upscaling[19] to generate upscaled absolute permeabilities on a 5×11×17 grid. Regression on the fine-grid results[20] was used to generate a single set of effective relative permeabilities, which ensured a good match to the fine grid.

Coats upscaled the 60×220×85 geostatistical grid to a 30×55×85 grid of 40×40×2-ft coarse gridblocks. The results of a model run for that grid were considered correct for the purpose of further flow-based upscaling. The 60×220×85 grid was upscaled to 10×20×10 and 3×5×5 coarse grids. The coarse blocks of the 10×20×10 grid were 120×110×14 ft in the Tarbert (120×110×20 ft in the Upper Ness). Those of the 3×5×5 grid were 400×440×34 ft. Coats reported three sets of results: the 30×55×85 grid, the 10×20×10 grid with a pseudo $k_{rw}=S_{wn}^{1.28}$, and the 3×5×5 grid with a pseudo $k_{rw}=S_{wn}^{1.2}$.

Phillips first upscaled the 60×220×85 grid, 1.122-million-cell geological model using a flow-based method[19] to a 31×55×85 grid containing 40×40-ft square areal grids except for rows 27, 28, and 29, where $\Delta Y=50$, 60, and 50 ft, respectively. This approach results in a fairly uniform grid across the field, including well cells, which are located in the center of their corresponding gridblocks. Peaceman's equation[19] was used to calculate the productivity index for each layer in the well. Simulation results from this fine-grid model were used as the basis for developing the coarse-grid upscaled model for use in the full-field model. The million-cell geological model was used directly to upscale to an 11×19×11 coarse-grid model for use in field-scale simulations. Pseudoization of the coarse-grid results to match the fine-grid calculations was performed by varying the Corey-type relative permeability exponents. Values of 1.6 for n_w and 2.4 for n_o were obtained.

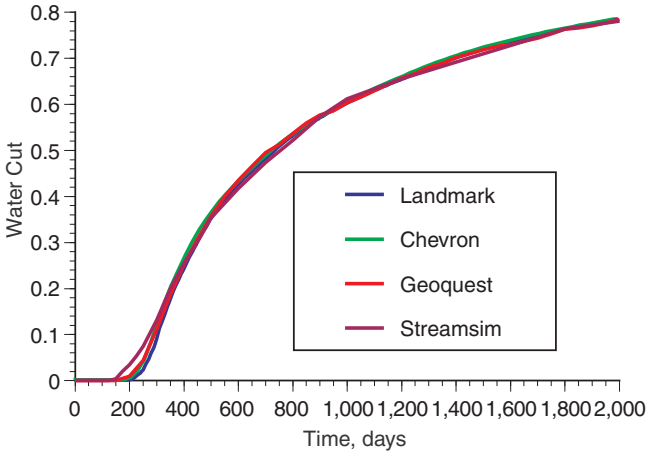

Fig. 9—Comparison of fine-grid Producer 1 water cut, Model 2.

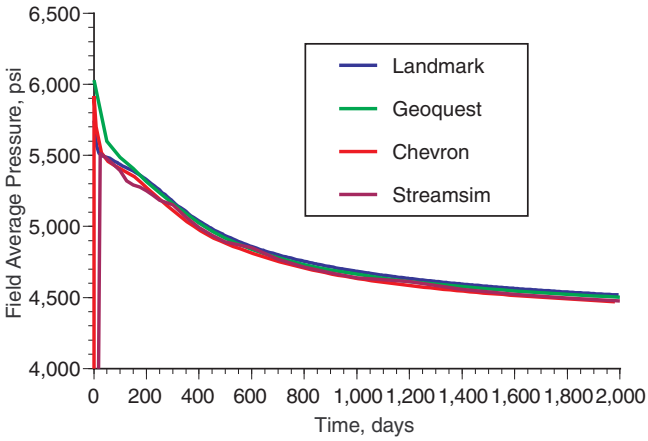

Fig. 10—Comparison of fine-grid field average pressure, Model 2.

Chevron used single-phase, flow-based upscaling in conjunction with a 3D nonuniform grid-coarsening code.[21] Although they had fine-scale model results available, these were not used in determining the grid or the upscaled properties. Instead, a single-phase tracer solution on both the fine and proposed coarse grids was compared, and the grid-coarsening strategy was varied to ensure reasonable agreement on quantities of interest such as breakthrough time. This resulted in a coarse grid size of 22×76×42.

TotalFinaElf adopted a similar strategy, using internal software to compute a coarsened grid. This software performs tracer flow simulations on the fine grid and on a series of coarse grids. A pressure gradient is imposed across the reservoir, with injection on one side and production on the other. Incompressible, single-phase flow is assumed. Four criteria are used to assess the results of the simulations on a particular coarse grid: total flux across the reservoir, tracer breakthrough time, a measure of the spread of the produced tracer concentration curve, and a curve-fit coefficient (a measure of the difference from the fine-grid-produced tracer concentration curve). As the grids become coarser areally, there is a gradual degradation of their quality as measured by these criteria, but with no obvious breakpoint where the quality of the grid becomes suddenly worse. On the other hand, as the number of layers is reduced, the quality appears to decline rapidly when fewer than 13 layers are used (only nearly uniform grids were considered). As a result of these tests, it was decided to use a 10×37×13 grid, with five layers in the Tarbert and eight in the Ness. The quality criteria also suggested that using no-flow lateral boundary conditions in the upscaling of permeabilities would be better than using linear boundary conditions.

GeoQuest submitted solutions using the following methods on a 15×55×17 coarse grid, where each coarse block contains a subgrid of dimensions 4×4×5. Porosity was upscaled with the usual volume-weighted arithmetic average. Permeability was upscaled using the following upscaling methods.

- Arithmetic-harmonic
- Harmonic-arithmetic
- Power averaging (with power=10^6 to extract maximum permeability)
- No-side-flow boundary conditions
- Linear boundary conditions
- Half-block permeability

The fine-grid relative permeability curves were used in the coarse-grid simulations.

Streamsim used a combination of arithmetic and geometric upscaling only. They first used arithmetic upscaling on k_x and k_y and geometric upscaling on k_z to go from 60×220×85 to 60×220×17.

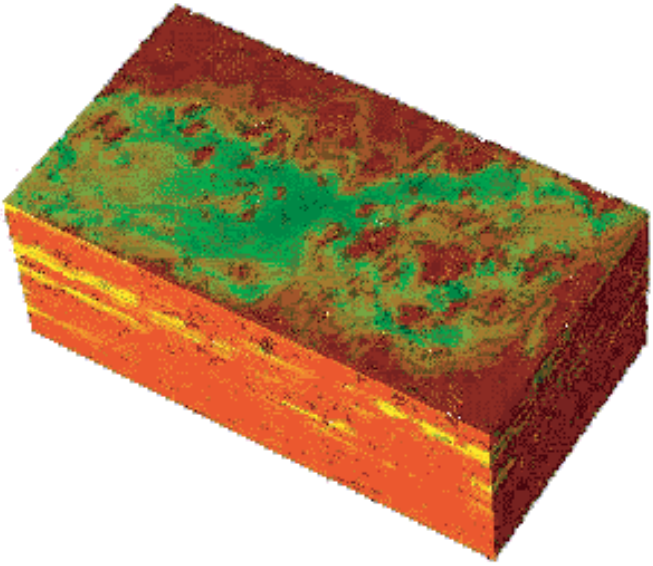

Fig. 11—TotalFinaElf fine-grid water saturation for Model 2 at 800 days using 3DSL.

All upscaling starting from 60×220×17 was then done with geometric upscaling only.

Roxar used layered sampling to map the 35 layers of the Tarbert onto nine layers of the upscaled model. The 50 layers of the Upper Ness were mapped onto 13 layers in the coarse grid, giving 22 layers in the z-direction (almost a factor of 4). The x- and y-directions were upscaled by a factor of 4 to 15 and 55 cells, respectively, giving a total of 18,150 global cells. A single discrete parameter was constructed on the fine grid, being the time of flight from the injector between 0 and 700 days. This parameter was upscaled to the coarse grid, where it was used to pick the cells to which 2×2×2 local grid refinements (LGR's) were applied. Some 3,120 LGR's were generated, giving a total of 39,990 active global and LGR cells. RMSsimgrid's single-phase diagonal tensor method was used to upscale the permeabilities, and the arithmetic average method was used to upscale the porosity onto this nonuniform grid.

Figs. 11 and 12 show fine- and coarse-grid water saturations computed with 3DSL by TotalFinaElf. Although much of the fine detail is missing from the coarse-grid solution, the overall shape of the saturation map is similar.

Fig. 13 shows field oil-production-rate results from all eight participants. The overall level of agreement is good, despite the fact that the methods use different grid sizes and simulators.

For a more detailed analysis, the results have been split into those that use pseudorelative permeabilities in some form and those that use only single-phase upscaling and upgridding, and the relative permeabilities have remained the same as the original rock curves.

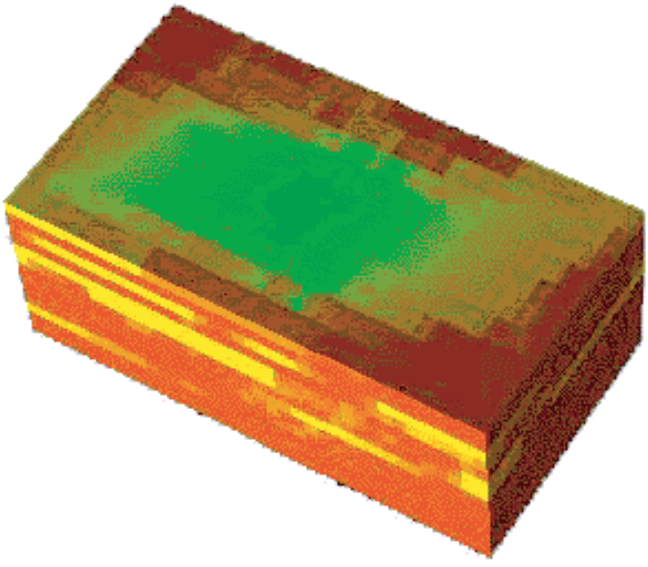

Fig. 12—TotalFinaElf coarse-grid water saturation for Model 2 at 800 days using 3DSL.

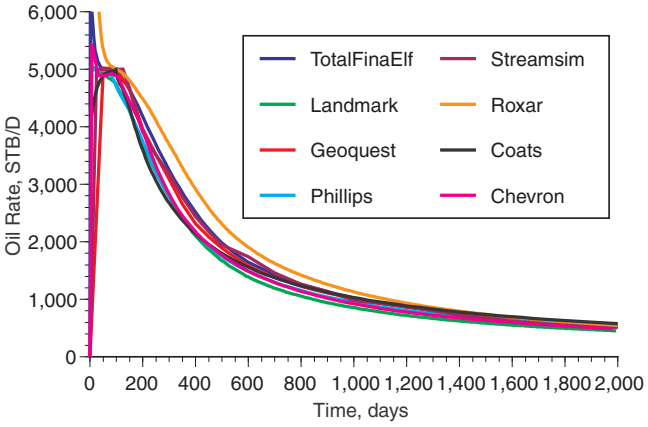

Fig. 13—Comparison of all field oil-rate curves for Model 2.

TABLE 1—SUMMARY OF ENTRIES FOR CASE 2

Company	Upscaling Method	Final Grid Size
GeoQuest	1. Arithmetic-harmonic 2. Harmonic-arithmetic 3. Power-law 4. Flow-based—no side flow 5. Flow-based—linear pressure 6. Flow-based—half cell	15×55×17 (14,025 cells)
Landmark	Flow-based, regression-based for relative permeabilities	5×11×17 (935 cells)
Roxar	Diagonal tensor	15×55×22 (39,990 total cells—global cells plus local refinements)
Streamsim	Geometric averaging	12×44×17 (8,976 cells) 30×110×17 30×110×85 60×220×17 60×220×85
Phillips	Single-phase to intermediate grid, regression on relative permeabilities to final grid	11×19×11 (2,299 cells)
TotalFinaElf	Upgridding and flow-based upscaling with no-side flow bcs	10×37×13 (4,810 cells)
Coats	Flow-based, regression-based pseudorelative permeabilities	30×55×85 10×20×10 (2,000 cells) 3×5×5
Chevron	Upgridding, flow-based upscaling	22×76×42 (70,224 cells)

The grid sizes used varied enormously. Table 1 includes information on grid sizes for each entry. For the pseudo-based approaches, grid sizes ranged from 75 cells (Coats) to 2,299 cells (Phillips). For the nonpseudo approaches, grid sizes varied from 4,810 cells (TotalFinaElf) to 70,224 cells (Chevron). For participants who submitted more than one entry, the entry plotted in the majority of curves is shown in bold in **Table 1.**

Generally, Producers 1 and 2 show the greatest variation between participants, with Producers 3 and 4 showing a higher level of agreement. We have chosen to show the Producer 1 results as well as the field totals to indicate the level of variability in the results.

We plotted the Landmark fine-grid solution as a reference fine-grid solution. Both Landmark and Chevron's fine-grid solutions are almost identical after the first 100 days of production, and differences before that time are almost certainly caused by different timestep strategies. The two streamline solutions are also very close after 150 days; therefore, we selected a single solution as a reference.

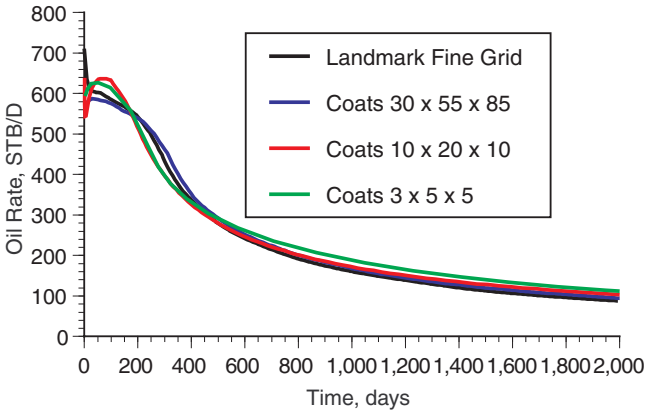

Fig. 15—Comparison of Coats' intermediate-grid solution with fine-grid and two coarse-grid solutions for oil rate for Producer 1.

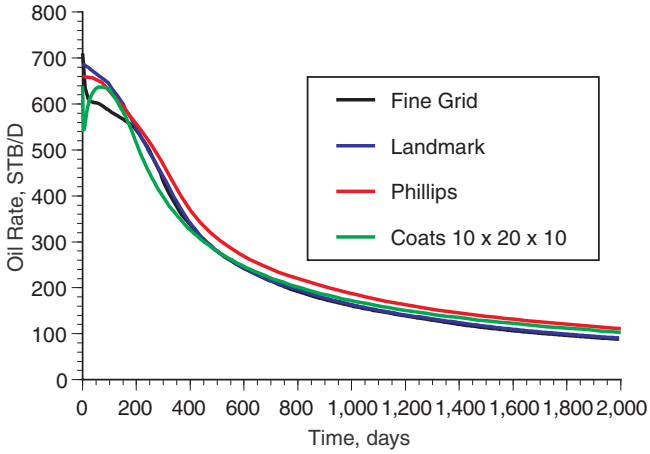

Fig. 14—Comparison of pseudo-based upscaled Producer 1 oil-rate curves with Landmark fine-grid oil rate for Model 2.

Fig. 14 shows the pseudo-based solutions for oil rate for Producer 1, along with the reference fine-grid solution. All solutions show some discrepancies at early times, then generally agree very well. The Landmark solution is the closest to the fine grid after 200 days, although it has the largest discrepancy in initial oil rate. Fig. 15 investigates the impact that pseudoization to an intermediate grid is likely to have had on the Coats and Phillips results. **Fig. 15** shows the Landmark fine-grid solution, along with the three solutions submitted by Coats: the 30×55×85 intermediate grid, and the 10×20×10 and 3×5×5 coarse grids. The intermediate grid solution is close to the true fine-grid solution and provides a good starting point for a pseudo-based approach. Both Coats upscaled solutions using pseudorelative permeabilities provide good predictions of the fine-grid results.

Fig. 16 shows an equivalent plot for the upscaling-based methods, where the relative permeabilities are left unchanged. Here, there is a significantly larger degree of scatter, reflecting the fact that knowledge of the fine-grid solution allows the relative permeabilities to be adjusted to give good agreement with the fine-grid solution. We plotted the no-flow boundary condition entry from GeoQuest in this plot and in all other comparative plots of upscaling entries. **Fig. 17** shows the results presented by GeoQuest to examine the variation in rate that can be predicted on a fixed grid (15×55×17) by changing the upscaling method. The worst method here is the use of linear pressure-gradient boundary conditions, which significantly overestimates the flow rate. This is in contrast to previously reported studies.[22] Both no-flow boundary conditions and arithmetic-harmonic averaging give good predictions.

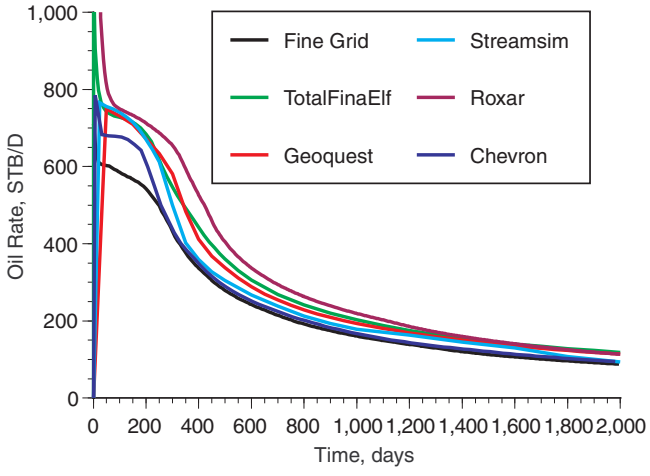

Fig. 16—Comparison of nonpseudo upscaled Producer 1 oil-rate curves with Landmark fine-grid oil rate for Model 2.

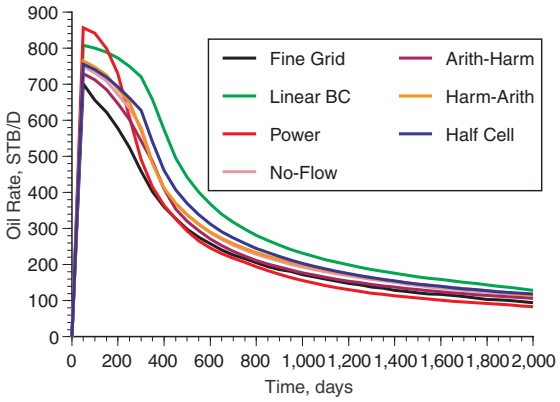

Fig. 17—Variation of Producer 1 oil rate with upscaling method for fixed coarse grid for Model 2.

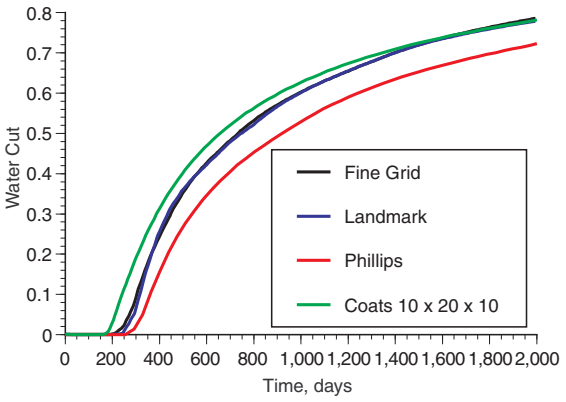

Fig. 18—Comparison of pseudo-based upscaled Producer 1 water-cut curves with Landmark fine-grid water cut for Model 2.

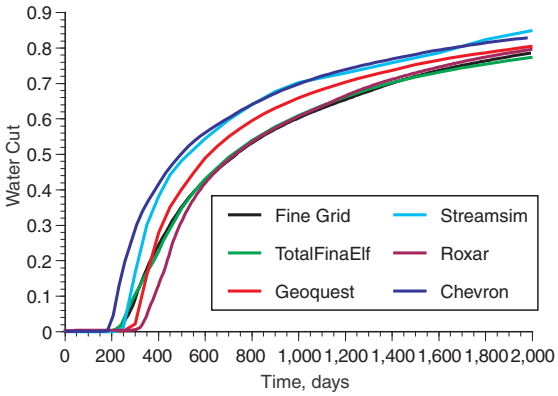

Fig. 19—Comparison of nonpseudo upscaled Producer 1 water-cut curves with fine-grid result for Model 2.

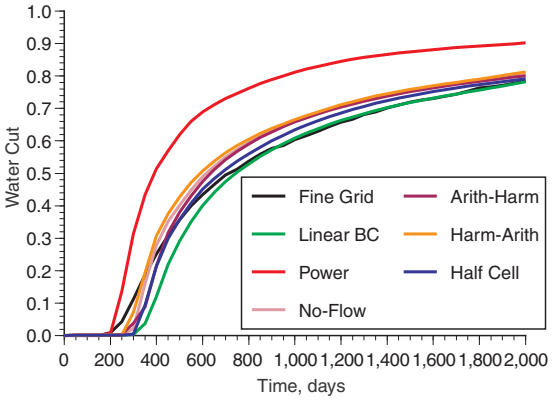

Fig. 20—Variation of Producer 1 water cut with upscaling method for fixed coarse grid for Model 2.

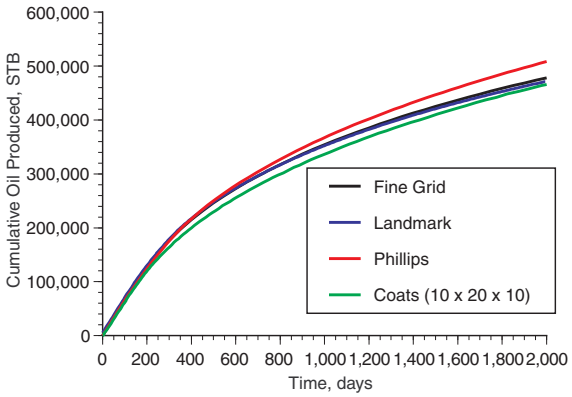

Fig. 21—Variation in cumulative oil production for Producer 1 for pseudo approaches.

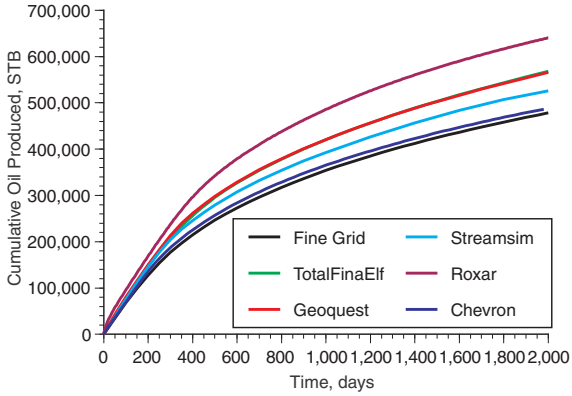

Fig. 22—Variation in cumulative oil production for Producer 1 for nonpseudo approaches.

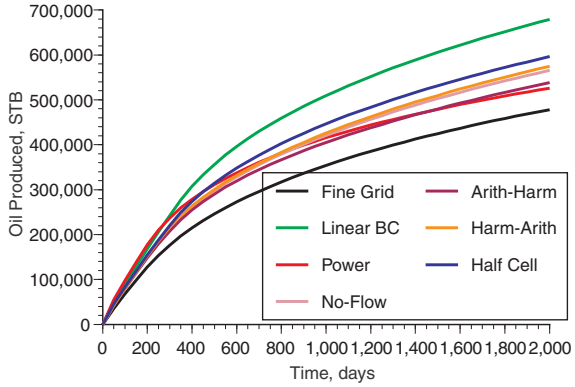

Fig. 23—Variation of cumulative oil produced for Producer 1 with upscaling method for fixed coarse grid for Model 2.

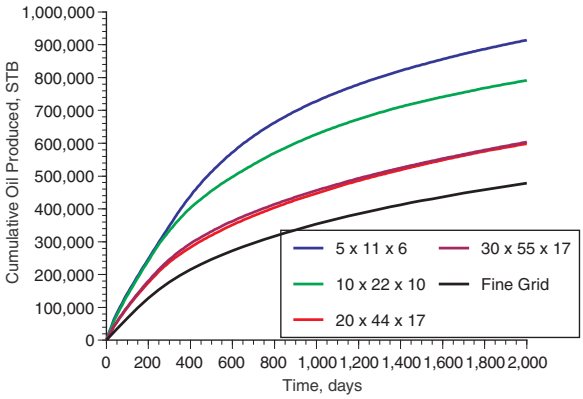

Fig. 24—Variation in cumulative oil production for Producer 1 with upscaled grid size.

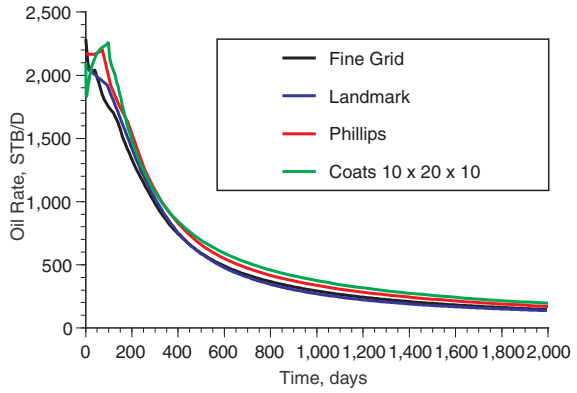

Fig. 25—Comparison of pseudo-based upscaled Producer 3 oil-rate curves with Landmark fine-grid oil rate for Model 2.

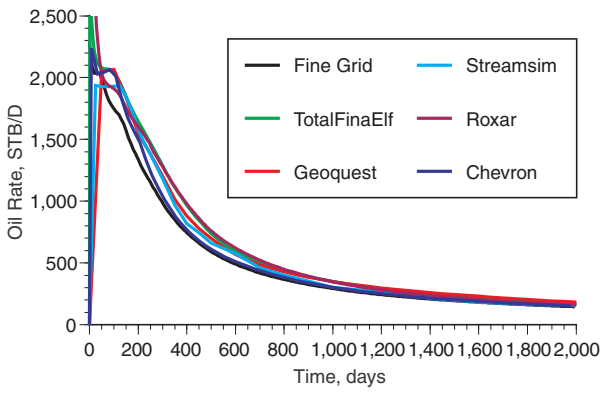

Fig. 26—Comparison of nonpseudo upscaled Producer 3 oil-rate curves with Landmark fine-grid oil rate for Model 2.

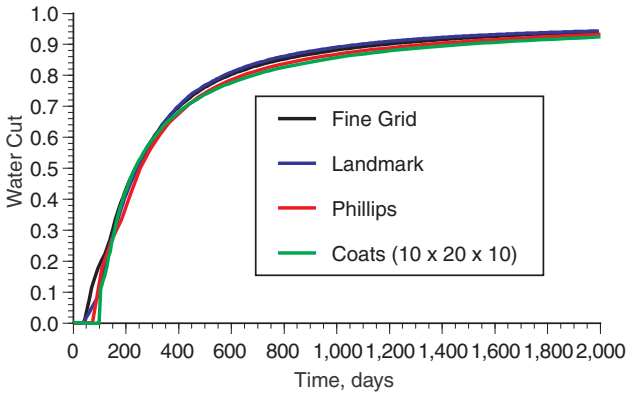

Fig. 27—Comparison of pseudo-based upscaled Producer 3 water-cut curves with Landmark fine-grid oil rate for Model 2.

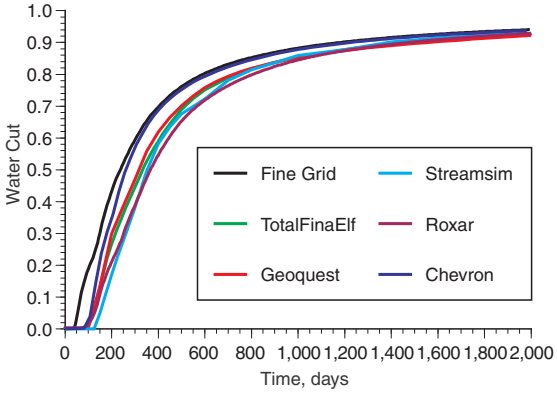

Fig. 28—Comparison of nonpseudo upscaled Producer 3 water-cut curves with Landmark fine-grid oil rate for Model 2.

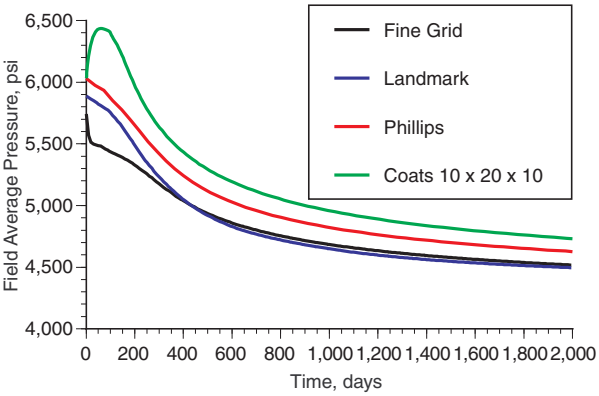

Fig. 29—Comparison of pseudo-based upscaled field average pressure curves with fine-grid field average pressure for Model 2.

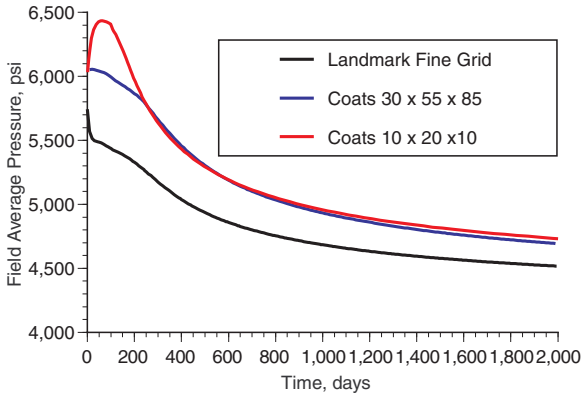

Fig. 30—Comparison of Coats' field average pressure curves for intermediate and coarse grids with fine grid for Model 2.

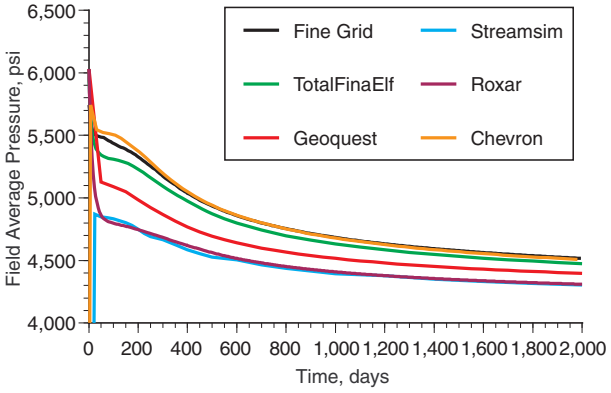

Fig. 31—Comparison of nonpseudo upscaled field average pressure curves with fine-grid result for Model 2.

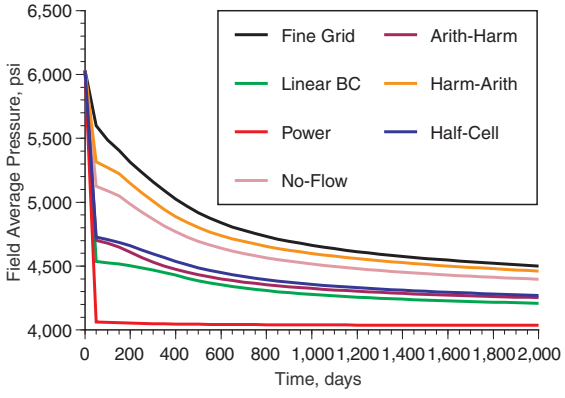

Fig. 32—Variation of field average pressure with upscaling method for fixed coarse grid for Model 2.

Figs. 18 through 20 show predictions of the water cut from Producer 1 for the same three groups of solutions. There is a slightly larger difference between the three pseudo-based approaches shown in Fig. 18. In Fig. 19, there is now a significant spread in predictions, with water breakthrough varying between 200 and just over 400 days. The variation in results owing to choice of method is again significant (Fig. 20), although now the power-law upscaling provides the worst prediction of water cut. Both no-flow boundary conditions and arithmetic-harmonic methods still provide good predictions.

Figs. 21 through 23 look at the prediction of cumulative oil produced for Producer 1. In Fig. 21, the pseudo-based methods all do a good job of predicting cumulative oil production. In Fig. 22, which shows the upscaling-based submissions, the Chevron solution is by far the closest, although it is also the most finely gridded solution. The others show the cumulative impact of errors in prediction at early times. Fig. 23 shows that the impact of upscaling techniques is as large as the spread between participants.

Because no participants submitted a very-coarse-grid solution using nonpseudo-based methods, we ran a set of cases at Heriot-Watt U. on grid sizes from 30×55×17 down to 5×11×6 using single-phase upscaling only. The coarsest grids used were of a size that might have been used if this were a pattern element in a full-field model. The upscaling method used was a pressure-solution technique with no-flow boundary conditions, so it was consistent with many participants' method of choice. The predictions were run with FRONTSIM, GeoQuest's streamline-based simulator. **Fig. 24** shows the predictions of cumulative oil production from Producer 1 with varying grid size. We can see that going to a coarse grid (of the size that might be used if the model here represented a pattern element of a full-field model) induces large errors. Interestingly, there is little difference between the 20×44×17 and the 30×55×17 predictions, but both are some way away from the fine-grid solution.

Figs. 25 through 28 show the variation in predictions for both oil rate and water cut for Producer 3, which is the largest producer. The results are much closer here than for Producer 1, although there are still reasonable errors in prediction of water breakthrough time.

The final set of results, **Figs. 29 through 32,** shows the predictions of field average pressure. The differences between the pseudo-based methods and the upscaling methods are less apparent here, with approximately the same level of variation between the two groups (Figs. 29 and 31). However, part of this variation is caused by the difference in field average pressure computed on the intermediate grid used by Coats and Phillips (Fig. 30). In Fig. 32, we can see that the closest pressure prediction is provided by the harmonic-arithmetic average, with no-flow boundary conditions close behind. The power law method (which selected only the maximum permeability here) clearly overestimates the effective permeability of the system and predicts a field average pressure that is too low.

Because this problem has low compressibility, the quality of the water- and oil-rate predictions is almost independent of the quality of the field average pressure prediction. As long as the upscaling method correctly estimates the ratios of the four producer productivity indices, the production split between the wells will be correct. However, field average pressure is determined by both the absolute values of the well productivity indices (PI's) and the pressure drop between the wells, so it is sensitive to estimating the correct absolute value of the well PI. This sensitivity to the well PI also has implications for the fine-grid field average pressure. If the wells had been moved a small distance, the well PI's might have changed significantly, and hence the computed fine-grid field average pressure is potentially sensitive to small changes in the well locations.

To aid future comparisons, the companies involved in this project have agreed to make their solutions available electronically. Spreadsheets containing the raw data for the line graphs can be downloaded from http://www.spe.org/csp.

Conclusions

The fine-grid results were all in good agreement. This was true for both Model 1, where computing the fine grid was easy, and for Model 2, which was significantly more time-consuming.

Model 1 was a relatively easy problem, and all participants were able to obtain coarse-grid solutions that agreed well with their own fine-grid results. These results were obtained mostly by a history-matching process to compute coarse-grid relative permeabilities. Roxar showed that it was also possible to obtain good results using only single-phase upscaling and local grid refinement, and Coats showed that it was possible to obtain a good match with a homogeneous permeability and the original rock curves on a coarse grid.

For Model 2, the fine-grid streamline simulations submitted by GeoQuest and Streamsim were in very good agreement with the fine-grid finite-difference solutions submitted by Landmark and Chevron. In addition, the intermediate-grid solutions submitted by Phillips and Coats were very close to the full fine-grid solutions, except for the field average pressure.

Where the fine grid can be run, a regression approach to pseudoization can give good agreement with the fine-grid results. Upscaling approaches where only the absolute permeability was averaged gave more scatter, though overall agreement on rate is generally good.

There was more scatter on prediction of individual well rates. This was true for both pseudoization approaches and upscaling approaches.

At the grid sizes submitted, there was as much variation in results owing to the choice of upscaling method as there was variation between individual solutions.

The coarse-grid solutions from Heriot-Watt U. showed that there was potential for significant errors caused by excessive grid coarsening if only single-phase upscaling is used.

Use of linear pressure-gradient boundary conditions was not a good choice for the model considered here. This is in contrast to other geological models where linear-pressure boundary conditions have resulted in a significant improvement in upscaling.

The best overall single-phase method in this case was flow-based upscaling using no-flow boundary conditions.

Accurate calculation of field average pressure is not a good measure of accuracy of oil- or water-rate prediction in this problem. The accuracy with which field average pressure is calculated is significantly influenced by the calculation of the upscaled well PI's.

Nomenclature

B = formation volume factor, bbl/bbl
c = compressibility, Lt^2m^{-1}, psi^{-1}
k = absolute permeability, L^2, Darcy
k_r = relative permeability
n = power in relative permeability expression
p = pressure, $m/L^{-1}t^{-2}$, psi
S = saturation
ϕ = porosity
μ = viscosity, $m/L^{-1}t^{-1}$, cp
ρ = density, m/L^{-3}, lb/ft^3

Subscripts

c = connate
g = gas
H = horizontal
i = initial
n = normalized
o = oil
r = residual
V = vertical
w = water

Acknowledgments

We wish to thank all the participants in this study for their time and results, without which this study would not have been possible. We also wish to thank several of the participants for constructive feedback on the first draft of this paper, and particularly Keith Coats for a useful discussion of the average pressure results. Thanks are also due to Nasir Darman for his help in setting up Model 1.

References

1. Odeh, A.: "Comparison of Solutions to a 3D Black-Oil Reservoir Simulation Problem," *JPT* (January 1981) 13; *Trans.,* AIME, **271.**
2. Weinstein, H.G., Chappelear, J.E., and Nolen, J.S.: "Second Comparative Solution Project: A Three-Phase Coning Study," *JPT* (March 1986) 345.
3. Kenyon, D.E. and Behie, G.A.: "Third SPE Comparative Solution Project: Gas Cycling of Retrograde Condensate Reservoirs," *JPT* (August 1987) 981.
4. Aziz, K., Ramesh, A.B., and Woo, P.T.: "Fourth SPE Comparative Solution Project: A Comparison of Steam Injection Simulators," *JPT* (December 1987) 1576.
5. Killough, J. and Cossack, C.: "Fifth Comparative Solution Project: Evaluation of Miscible Flood Simulators," paper SPE 16000 presented at the 1987 SPE Symposium on Reservoir Simulation, San Antonio, Texas, 1–4 February.
6. Firoozabadi, A. and Thomas, L.K.: "Sixth SPE Comparative Solution Project: Dual Porosity Simulators," *JPT* (June 1990) 710.
7. Nghiem, L., Collins, D.A., and Sharma, R.: "Seventh SPE Comparative Solution Project: Modeling of Horizontal Wells in Reservoir Simulation," paper SPE 21221 presented at the 1991 SPE Symposium on Reservoir Simulation, Anaheim, California, 17–20 February.
8. Quandalle, P.: "Eighth SPE Comparative Solution Project: Gridding Techniques in Reservoir Simulation," paper SPE 25263 presented at the 1993 SPE Symposium on Reservoir Simulation, New Orleans, 28 February–3 March.
9. Killough, J.: "Ninth SPE Comparative Solution Project: A Reexamination of Black-Oil Simulation," paper SPE 29110 presented at the 1995 SPE Symposium on Reservoir Simulation, San Antonio, Texas, 12–15 February.
10. Web site for the 10th SPE Comparative Solution Project: http://www.spe.org/csp/.
11. Renard, Ph. and de Marsily, G.: "Calculating Equivalent Permeability: A Review," *Advances in Water Resources* (1997) **20,** Nos. 5–6, 253.
12. Barker, J.W. and Thibeau, S.: "A Critical Review of the Use of Pseudorelative Permeabilities for Upscaling," *SPERE* (May 1997) 109.
13. Barker, J.W. and Dupouy, Ph.: "An Analysis of Dynamic Pseudo Relative Permeability Methods," *Petroleum Geoscience* (1999) **5,** No. 4, 385.
14. Christie, M.A.: "Upscaling for Reservoir Simulation," *JPT* (November 1996) 1004.
15. Floris, F.J.T. *et al.:* "Comparison of production forecast uncertainty quantification methods—an integrated study," 1999 Conference on Petroleum Geostatistics, Toulouse, France, 20–23 April. See also the PUNQ Web site, http://www.nitg.tno.nl/punq/.
16. Lolomari, T. *et al.:* "The Use of Streamline Simulation in Reservoir Management Methodology and Case Studies," paper SPE 63157 presented at the 2000 SPE Annual Technical Conference and Exhibition, Dallas, 1–4 October.
17. Batycky, R.P., Blunt, M.J., and Thiele, M.R.: "A 3D Field-Scale Streamline-Based Reservoir Simulator," *SPERE* (November 1997) 246.
18. Qi, D., Wong, P.M., and Liu, K.: "An Improved Global Upscaling Approach for Reservoir Simulation," *Pet. Sci. & Tech.* (2001) **19,** No. 7–8.
19. Peaceman, D.W.: "Effective Transmissibilities of a Gridblock by Upscaling—Why Use Renormalization?" paper SPE 36722 presented at the 1996 SPE Annual Technical Conference and Exhibition, Denver, Colorado, 6–9 October.
20. Johnson, J.B. *et al.:* "The Kuparuk River Field: A Regression Approach to Pseudorelative Permeabilities," paper SPE 10531 presented at the 1982 SPE Symposium on Reservoir Simulation, New Orleans, 31 January–3 February.
21. Durlofsky, L.J. *et al.:* "Scaleup of Heterogeneous 3D Reservoir Descriptions," paper SPE 30709 presented at the 1995 SPE Annual Technical Conference and Exhibition, Dallas, 22–25 October.
22. King, M.J. and Mansfield, M.: "Flow Simulation of Geologic Models," paper SPE 38877 presented at the 1997 SPE Annual Technical Conference and Exhibition, San Antonio, Texas, 5–8 October.

Appendix A—Details of Model 1

The model is a two-phase (oil and gas) model that has a simple 2D vertical cross-sectional geometry with no dipping or faults. The dimensions of the model are 2,500 ft long×25 ft wide×50 ft thick. The fine-scale grid is 100×1×20, with uniform size for each of the gridblocks. The top of the model is at 0.0 ft, with initial pressure at this point of 100 psia. Initially, the model is fully saturated with oil (no connate water).

The initial properties of the fine-grid model are as follows: $\phi=0.2$; gridblock sizes DX=25 ft, DY=25 ft, and DZ=2.5 ft; $\mu_o=1$ cp and $\mu_g=0.01$ cp (constant throughout the run); and $\rho_o=43.68$ lb/ft^3, and $\rho_g=0.0624$ lb/ft^3.

The permeability distribution is a correlated, geostatistically generated field (log k is shown in Fig. 1). The permeability field and the relative permeabilities were downloaded from the project Web site.

The fluids are assumed to be incompressible and immiscible. The fine-grid relative permeabilities are shown in Fig. 2. Capillary pressure was assumed to be negligible in this case. Gas was injected from an injector located at the left of the model, and dead oil was produced from a well to the right of the model.

Both wells have a well internal diameter of 1.0 ft and are completed vertically throughout the model. The injection rate was set to give a frontal velocity of 1 ft/D (about 0.3 m/d or 6.97 m^3/d), and the producer is set to produce at a constant bottomhole pressure limit of 95 psia. The reference depth for the bottomhole pressure is at 0.0 ft (top of the model).

Appendix B—Details of Model 2

This model has a sufficiently fine grid to make the use of classical pseudoization methods almost impossible. The model has a simple geometry, with no top structure or faults. The reason for this choice is to provide maximum flexibility in the choice of upscaled grids.

At the fine geological model scale, the model is described on a regular Cartesian grid. The model dimensions are 1,200×2,200×170 ft. The top 70 ft (35 layers) represent the Tarbert formation, and the bottom 100 ft (50 layers) represent Upper Ness. The fine-scale cell size is 20×10×2 ft. The model consists of part of a Brent sequence. The model was originally generated for use in the PUNQ project. The top part of the model is a Tarbert formation and is a representation of a prograding near-shore environment. The lower part (Upper Ness) is fluvial.

Fig. 3 shows the porosity for the whole model. The fine-scale model size is 60×220×85 cells (1.122×10^6 cells). The porosity and permeability maps were downloaded from the project Web site.

Water properties are $B_w=1.01$, $c_w=3.10^{-6}$ psi^{-1}, and $\mu_w=0.3$ cp. The dead-oil pressure/volume/temperature (PVT) data are shown in **Table B-1.**

Relative permeabilities are

$$k_{rw}=\left(\frac{S-S_{wc}}{1-S_{wc}-S_{or}}\right)^2, \quad \ldots\ldots\ldots\ldots\ldots\ldots\ldots\ldots\ldots \text{(B-1)}$$

$$k_{ro}=\left(\frac{1-S-S_{or}}{1-S_{wc}-S_{or}}\right)^2, \quad \ldots\ldots\ldots\ldots\ldots\ldots\ldots\ldots\ldots \text{(B-2)}$$

and $S_{wc}=S_{wi}=S_{or}=0.2$. $\ldots\ldots\ldots\ldots\ldots\ldots\ldots\ldots\ldots$ (B-3)

All wells were vertical and completed throughout the formation. The central injector has an injection rate of 5,000 B/D (reservoir conditions) and a maximum injection bottomhole pressure of 10,000 psi. There are four producers in the four corners of the model; each produces at 4,000 psi bottomhole pressure.

TABLE B-1—DEAD-OIL PVT DATA

p (psi)	B_o	μ_o
300	1.05	2.85
800	1.02	2.99
8,000	1.01	3.0

SI Metric Conversion Factors

ft × 3.048*	E − 01 = m
ft^3 × 2.831 685	E − 02 = m^3
lbm × 4.535 924	E − 01 = kg

*Conversion factor is exact. **SPEREE**

Michael A. Christie is Professor of Reservoir Engineering at Heriot-Watt U., Edinburgh, U.K. e-mail: mike.christie@pet.hw.ac.uk. Previously, he worked for 18 years for BP Research and BP Exploration, holding positions in technology in the U.K. and the U.S. His research interests are uncertainty estimation, upscaling, and numerical methods. He holds a BS degree in mathematics and a PhD degree in plasma physics, both from the U. of London. Christie has served on the organizing committee of the SPE Reservoir Simulation Symposium and is a technical editor for *SPE Reservoir Evaluation and Engineering.* He was awarded the 1990 Cedric K. Ferguson Medal, and he served as a Distinguished Lecturer from 1994–95. **Martin J. Blunt** is Professor of Petroleum Engineering and head of the Petroleum Engineering and Rock Mechanics Research Group at Imperial College, London. e-mail: m.blunt@ic.ac.uk. He previously was an associate professor at Stanford U. and worked at the BP Research Centre. He holds MA and PhD degrees in physics from Cambridge U. Blunt, winner of the 1996 Cedric K. Ferguson Medal, served as Associate Executive Editor of *SPE Journal* from 1996–98. He currently is a member of the *SPE Journal* Editorial Board, a faculty adviser for the Imperial College SPE Student Chapter, and a member of the Program Committees for the Improved Oil Recovery Symposium and the Reservoir Simulation Symposium. Blunt is a 2001 Distinguished Lecturer.